Undamped collective surface plasmon oscillations along metallic nanosphere chains

W. Jacak,[1,a)] J. Krasnyj,[1,2] J. Jacak,[1] A. Chepok,[2] L. Jacak,[1] W. Donderowicz,[1] D. Z. Hu,[3] and D. M. Schaadt[3]
[1]*Institute of Physics, Wrocław University of Technology, Wyb. Wyspiańskiego 27, 50-370, Wrocław, Poland*
[2]*Theor. Phys. Group, International University, Fontanskaya Doroga 33, Odessa 65-026, Ukraine*
[3]*Institute of Applied Physics/DFG-Center for Functional Nanostructures, Karlsruhe Institute of Technology, Weberstrasse 5, 76-133 Karlsruhe, Germany*

(Received 14 July 2010; accepted 25 August 2010; published online 19 October 2010)

The random-phase-approximation semiclassical scheme for describing plasmon excitations in large metallic nanospheres (with radius ~10–60 nm) is developed for the case when a dynamical electric field is present. The spectrum of plasmons in metallic nanospheres is determined including both surface and volume-type excitations and their mutual connections. It is demonstrated that only dipole-type surface plasmons can be excited by a homogeneous dynamical electric field. The Lorentz friction due to irradiation of electromagnetic energy by plasmon oscillations is analyzed with respect to sphere dimension. The resulting shift in resonance frequency due to plasmon damping is compared with experimental data for various sphere radii. Wave-type collective oscillations of surface plasmons in long chains of metallic nanospheres are described. The undamped region for collective plasmon propagation along the metallic chain is found in agreement with previous numerical simulations. © *2010 American Institute of Physics*.
[doi:10.1063/1.3493263]

I. INTRODUCTION

Experimental and theoretical invesitigations of plasmon excitations in metallic nanocrystals rapidly grew mainly due to possible applications in photovoltaics and microelectronics. A significant enhancement of absorption of incident light in photodiode-systems with an active surface covered with nanodimension metallic particles (of Au, Ag, or Cu) with planar density $\sim 10^8-10^{10}/\mathrm{cm}^2$ was observed.[1–7] This is due to a mediating role in light energy transport carried out by surface plasmon oscillations in metallic nanocompounds on a semiconductor surface. These findings are of practical importance for enhancement of solar cell efficiency, especially for thin film cell technology. On the other hand, hybridized states of surface plasmons and photons result in plasmon-polaritons[8] which are of high importance for applications in photonics and microelectronics,[9,10] in particular, for transportation of energy in metallic modified structures in nanoscale.[11,12]

Surface plasmons in nanoparticles have been widely investigated since their classical description by Mie.[13] Many particular studies, including numerical modeling of multielectron clusters, have been carried out.[14–18] They were mostly developments of Kohn–Sham attitude in form of local density approximation (LDA) or time dependent LDA (TDLDA) (Refs. 14–17) for small metallic clusters only, up to approximately 200 electrons (as limited by numerical calculation constraints that grow rapidly with the number of electrons). The random-phase-approximation (RPA) was formulated[19] for description of volume plasmons in bulk metals and utilized also for confined geometry mainly in a numerical or seminumerical manner.[16] Usually, in these analyses the *jellium* model was assumed for description of positive ion background in the metal and dynamics was addressed to the electron system only.[16–18] Such an attitude is preferable for clusters of simple metals, including noble metals (also transition and alkali metals). It should be noted, however, that the TDLDA approach was successfully applied to nanoshells with radius above 10 nm and thickness up to a few nanometers[20] via acceleration of the numerical procedures. It was achieved by assuming screened effective Coulomb interaction, which enhanced convergence of iterations, thus allowing for effective solution of Kohn–Sham type equations for even more than 10^4 electrons within a jellium model. For the nanoshell systems also numerical solution of the RPA-type polarization self-consistent equation has been found.[21] These analyses showed that plasmon resonances in nanoshells are similar to classical Mie-type ones, redshifted, however, with respect to them, similarly as it was for small clusters (mostly due to spill-out of electrons beyond the jellium rim). The radiation effects were not included, corresponding to not severe contribution of radiation losses even for relatively large radius of nanoshells, because the number of electrons in a shell is much lower than in a full nanosphere of similar radius. One can thus expect that dimension scaling of radiation losses, being of cubic type for nanospheres,[22] does not apply to shells, resulting in the overall shift in radiation effects in shells to larger radius region in comparison to full spheres (likely, above the radii considered in Refs. 20 and 21).

In the present paper we generalize the bulk RPA description,[19] using a semiclassical approach for a large metallic nanosphere (with radius of several tens of nanometers

a)Electronic mail: lucjan.jacak@pwr.wroc.pl.

and with 10^5-10^7 electrons) in an all-analytical calculus version.[22] The electron liquid oscillations of compressional and translational type result in excitations inside the sphere and on its surface, respectively. They are analyzed and referred to as volume and surface plasmons. Damping of plasmons due to electron scattering (nonlocal processes) and due to radiation losses (retardation effects accounted for via the Lorentz friction force) is included. The shift in the resonance frequency of dipole-type surface plasmons (only such plasmons are induced by homogeneous time-dependent electric field), due to damping phenomena, is compared with the experimental data for various nanosphere radii.

Collective surface dipole-type plasmon oscillations in the linear chain of metallic nanospheres are analyzed and wave-type plasmon modes are described. A coupling in the near-field regime between oscillating dipoles of surface plasmons, together with retardation effects for energy irradiation, lead to the possibility of undamped propagation of plasmon waves along the chain in the experimentally realistic region of parameters (separation of spheres in the chain and their radii). These effects are of particular significance for plasmon arranged nondissipative transport of energy along metallic chains for application in nanoelectronics.

In Sec. II of this paper, the standard RPA theory in the quasiclassical limit, is generalized for a confined system of spherical shape. The resulting equations for volume and surface plasmons are solved in the following section (with the particularities of calculus shifted to the Appendix). Section III contains a description of the Lorentz friction for surface plasmons oscillations of the dipole-type. Analysis of collective wave-type surface plasmon oscillations in a chain of metallic nanospheres is presented in Sec. V. Besides the theoretical model the comparison of the characteristic nanoscale plasmon behavior with available experimental data, including our own measurements, is presented.

II. RPA APPROACH TO ELECTRON EXCITATIONS IN METALLIC NANOSPHERE

A. Derivation of RPA equation for local electron density in a confined spherical geometry

Let us consider a metallic sphere with radius a located in vacuum, $\varepsilon=1$, $\mu=1$ and in the presence of dynamical electric field (magnetic field is assumed to be zero). We will consider collective electrons in the metallic material. The model jellium[16–18] is assumed in order to account for the screening background of positive ions in the form of static positive charge uniformly distributed over the sphere

$$n_e(\boldsymbol{r}) = n_e\Theta(a-r), \tag{1}$$

where $n_e=N_e/V$ and $n_e|e|$ is the averaged positive charge density, N_e is the number of collective electrons in the sphere, $V=(4\pi a^3/3)$ is the sphere volume, and Θ is the Heaviside step-function. Neglecting ion dynamics within the jellium model, which is adopted in particular for description of simple metals, e.g., noble, transition, and alkali metals, we deal with the Hamiltonian for collective electrons,

$$\hat{H}_e = \sum_{j=1}^{N_e}\left[-\frac{\hbar^2\nabla_j^2}{2m} - e^2\int\frac{n_e(\boldsymbol{r}_0)d^3\boldsymbol{r}_0}{|\boldsymbol{r}_j-\boldsymbol{r}_0|} + e\varphi(\boldsymbol{R}+\boldsymbol{r}_j,t)\right] + \frac{1}{2}\sum_{j\neq j'}\frac{e^2}{|\boldsymbol{r}_j-\boldsymbol{r}_{j'}|} + \Delta E, \tag{2}$$

where $\boldsymbol{r}_j$ and m are the position (with respect to the sphere center) and the mass of the jth electron, respectively, $\boldsymbol{R}$ is the position of the metallic sphere center, ΔE represents electrostatic energy contribution from the ion "jellium," and $\varphi(\boldsymbol{r},t)$ is the scalar potential of the external electric field. The corresponding electric field $\boldsymbol{E}(\boldsymbol{R}+\boldsymbol{r}_j,t)=-\mathrm{grad}_j\varphi(\boldsymbol{R}+\boldsymbol{r}_j,t)$. Assuming that the space-dependent variation in $\boldsymbol{E}$ is weak on the scale of the sphere radius a, then $\boldsymbol{E}(\boldsymbol{R}+\boldsymbol{r}_j,t)\simeq\boldsymbol{E}(\boldsymbol{R},t)$, i.e., the electric field is homogeneous over the sphere. Then $\varphi(\boldsymbol{R}+\boldsymbol{r}_j,t)\simeq-\boldsymbol{E}(\boldsymbol{R},t)\cdot\boldsymbol{R}+\varphi_1(\boldsymbol{R}+\boldsymbol{r}_j,t)$, where $\varphi_1(\boldsymbol{R}+\boldsymbol{r}_j,t)=-\boldsymbol{r}_j\cdot\boldsymbol{E}(\boldsymbol{R},t)$. Hence, one can rewrite the Hamiltonian (2) in the form

$$\hat{H}_e = \hat{H}_e' - eN\boldsymbol{E}(\boldsymbol{R},t)\cdot\boldsymbol{R}, \tag{3}$$

where

$$\hat{H}_e' = \sum_{j=1}^{N_e}\left[-\frac{\hbar^2\nabla_j^2}{2m} - e^2\int\frac{n_e(\boldsymbol{r})d^3\boldsymbol{r}_0}{|\boldsymbol{r}_j-\boldsymbol{r}_0|} + e\varphi(\boldsymbol{r}_j,t)\right] + \frac{1}{2}\sum_{j\neq j'}\frac{e^2}{|\boldsymbol{r}_j-\boldsymbol{r}_{j'}|} + \Delta E, \tag{4}$$

and the corresponding (to $\hat{H}_e$) wave function can be represented as,

$$\Psi(\boldsymbol{r}_e,t) = \Psi'(\boldsymbol{r}_e,t)e^{i(eN/\hbar)\int\boldsymbol{E}(\boldsymbol{R},t)\cdot\boldsymbol{R}dt}, \tag{5}$$

with $i\hbar\,\partial\Psi'/\partial t=\hat{H}_e'\Psi'$, $\boldsymbol{r}_e=(\boldsymbol{r}_1,\boldsymbol{r}_2,\ldots,\boldsymbol{r}_N)$.

A local electron density can be written as follows:[19]

$$\rho(\boldsymbol{r},t) = \langle\Psi(\boldsymbol{r}_e,t)|\sum_j\delta(\boldsymbol{r}-\boldsymbol{r}_j)|\Psi(\boldsymbol{r}_e,t)\rangle = \langle\Psi'(\boldsymbol{r}_e,t)|\sum_j\delta(\boldsymbol{r}-\boldsymbol{r}_j)|\Psi'(\boldsymbol{r}_e,t)\rangle, \tag{6}$$

with the Fourier picture

$$\tilde{\rho}(\boldsymbol{k},t) = \int\rho(\boldsymbol{r},t)e^{-i\boldsymbol{k}\cdot\boldsymbol{r}}d^3r = \langle\Psi'(\boldsymbol{r}_e,t)|\hat{\rho}(\boldsymbol{k})|\Psi'(\boldsymbol{r}_e,t)\rangle, \tag{7}$$

where the "operator" $\hat{\rho}(\boldsymbol{k})=\Sigma_j e^{-i\boldsymbol{k}\cdot\boldsymbol{r}_j}$.

Using the above notation one can rewrite $\hat{H}_e'$ in the following form, in analogy to the bulk case[23]

$$\hat{H}_e' = \sum_{j=1}^{N_e}\left[-\frac{\hbar^2\nabla_j^2}{2m}\right] - \frac{e^2}{4\pi^2}\int d^3k\tilde{n}_e(\boldsymbol{k})\frac{1}{k^2}[\hat{\rho}^+(\boldsymbol{k})+\hat{\rho}(\boldsymbol{k})] + \frac{e^2}{16\pi^3}\int d^3k\tilde{\varphi}_1(\boldsymbol{k},t)[\hat{\rho}^+(\boldsymbol{k})+\hat{\rho}(\boldsymbol{k})] + \frac{e^2}{4\pi^2}\int d^3k\frac{1}{k^2}[\hat{\rho}^+(\boldsymbol{k})\hat{\rho}(\boldsymbol{k})-N_e] + \Delta E, \tag{8}$$

where $\tilde{n}_e(\boldsymbol{k})=\int d^3r n_e(\boldsymbol{r})e^{-i\boldsymbol{k}\cdot\boldsymbol{r}}$, $4\pi/k^2=\int d^3r 1/re^{-i\boldsymbol{k}\cdot\boldsymbol{r}}$, and $\tilde{\varphi}_1(\boldsymbol{k},t)=\int d^3r\varphi(\boldsymbol{r},t)e^{-i\boldsymbol{k}\cdot\boldsymbol{r}}$.

Utilizing this form of the electron Hamiltonian one can write the second time-derivative of $\hat{\rho}(\boldsymbol{k})$,

$$\frac{d^2\hat{\rho}(\boldsymbol{k},t)}{dt^2}=\frac{1}{(i\hbar)^2}\{[\hat{\rho}(\boldsymbol{k}),\hat{H}'_e],\hat{H}'_e\}, \tag{9}$$

which resolves itself into the equation

$$\begin{aligned}\frac{d^2\delta\hat{\rho}(\boldsymbol{k},t)}{dt^2}=&-\sum_j e^{-i\boldsymbol{k}\cdot\boldsymbol{r}_j}\left\{-\frac{\hbar^2}{m^2}(\boldsymbol{k}\cdot\nabla_j)^2+\frac{\hbar^2k^2}{m^2}i\boldsymbol{k}\cdot\nabla_j\right.\\&\left.+\frac{\hbar^2k^4}{4m^2}\right\}-\frac{e^2}{m2\pi^2}\int d^3q\tilde{n}_e(\boldsymbol{k}-\boldsymbol{q})\frac{\boldsymbol{k}\cdot\boldsymbol{q}}{q^2}\delta\hat{\rho}(\boldsymbol{q})\\&-\frac{e}{m8\pi^3}\int d^3q\tilde{n}_e(\boldsymbol{k}-\boldsymbol{q})(\boldsymbol{k}\cdot\boldsymbol{q})\tilde{\varphi}_1(\boldsymbol{q},t)\\&-\frac{e}{m8\pi^3}\int d^3q\,\delta\hat{\rho}(\boldsymbol{k}-\boldsymbol{q})(\boldsymbol{k}\cdot\boldsymbol{q})\tilde{\varphi}_1(\boldsymbol{q},t)\\&-\frac{e^2}{m2\pi^2}\int d^3q\,\delta\hat{\rho}(\boldsymbol{k}-\boldsymbol{q})\frac{\boldsymbol{k}\cdot\boldsymbol{q}}{q^2}\delta\hat{\rho}(\boldsymbol{q}),\end{aligned} \tag{10}$$

where $\delta\hat{\rho}(\boldsymbol{k})=\hat{\rho}(\boldsymbol{k})-\tilde{n}_e(\boldsymbol{k})$ is the operator of local electron density fluctuations beyond the uniform distribution. Taking into account that $\delta\tilde{\rho}(\boldsymbol{k},t)=\langle\Psi'(t)|\delta\hat{\rho}(\boldsymbol{k})|\Psi'(t)\rangle=\tilde{\rho}(\boldsymbol{k},t)-\tilde{n}_e(\boldsymbol{k})$, we find,

$$\begin{aligned}\frac{\partial^2\delta\tilde{\rho}(\boldsymbol{k},t)}{\partial t^2}=&\langle\Psi'|-\sum_j e^{-i\boldsymbol{k}\cdot\boldsymbol{r}_j}\left\{-\frac{\hbar^2}{m^2}(\boldsymbol{k}\cdot\nabla_j)^2+\frac{\hbar^2k^2}{m^2}i\boldsymbol{k}\cdot\nabla_j\right.\\&\left.+\frac{\hbar^2k^4}{4m^2}\right\}|\Psi'\rangle-\frac{e^2}{m2\pi^2}\int d^3q\tilde{n}_e(\boldsymbol{k}\\&-\boldsymbol{q})\frac{\boldsymbol{k}\cdot\boldsymbol{q}}{q^2}\delta\tilde{\rho}(\boldsymbol{q},t)-\frac{e}{m8\pi^3}\int d^3q\tilde{n}_e(\boldsymbol{k}-\boldsymbol{q})\\&\times(\boldsymbol{k}\cdot\boldsymbol{q})\tilde{\varphi}_1(\boldsymbol{q},t)-\frac{e}{m8\pi^3}\int d^3q\,\delta\tilde{\rho}(\boldsymbol{k}-\boldsymbol{q},t)\\&\times(\boldsymbol{k}\cdot\boldsymbol{q})\tilde{\varphi}_1(\boldsymbol{q},t)-\frac{e^2}{m2\pi^2}\int d^3q\frac{\boldsymbol{k}\cdot\boldsymbol{q}}{q^2}\langle\Psi'|\delta\hat{\rho}(\boldsymbol{k}\\&-\boldsymbol{q})\delta\hat{\rho}(\boldsymbol{q})|\Psi'\rangle.\end{aligned} \tag{11}$$

One can simplify the above equation with the assumption that $\delta\rho(\boldsymbol{r},t)=1/8\pi^3\int e^{i\boldsymbol{k}\cdot\boldsymbol{r}}\delta\tilde{\rho}(\boldsymbol{k},t)d^3k$ only weakly varies on the interatomic scale, and, therefore, three components of the first term on right-hand-side of Eq. (11) can be estimated as: $k^2v_F^2\delta\tilde{\rho}(\boldsymbol{k})$, $k^3v_F/k_T\delta\tilde{\rho}(\boldsymbol{k})$, and $k^4v_F^2/k_T^2\delta\tilde{\rho}(\boldsymbol{k})$, respectively, with $1/k_T$ the Thomas–Fermi radius,[19] $k_T=\sqrt{6\pi n_e e^2/\epsilon_F}$, ϵ_F is the Fermi energy, and v_F is the Fermi velocity. Thus, the contribution of the second and third components of the first term can be neglected in comparison to the first component. Also small, and thus negligible, is the last term on the right-hand-side of Eq. (11), as it involves a product of two $\delta\tilde{\rho}$ (which we assumed small $\delta\tilde{\rho}/n_e\ll 1$). This approach corresponds to RPA attitude formulated for bulk metal[19,23] [note that $\delta\hat{\rho}(0)=0$ and the coherent RPA contribution of interaction is contained in the second term in Eq. (11)]. The last but one term in Eq. (11) can also be omitted if one confines it to linear terms with respect to $\delta\tilde{\rho}$ and $\tilde{\varphi}_1$. Next, due to spherical symmetry, $\langle\Psi'|\Sigma_j e^{-i\boldsymbol{k}\cdot\boldsymbol{r}_j}(\hbar^2/m^2)(\boldsymbol{k}\cdot\nabla_j)^2|\Psi'\rangle\simeq(2k^2/3m)\times\langle\Psi'|\Sigma_j e^{-i\boldsymbol{k}\cdot\boldsymbol{r}_j}(\hbar^2\nabla_j^2/2m)|\Psi'\rangle$. Performing the inverse Fourier transform, Eq. (11) finally attains the form,

$$\begin{aligned}\frac{\partial^2\delta\rho(\boldsymbol{r},t)}{\partial,t^2}=&-\frac{2}{3m}\nabla^2\langle\Psi'|\sum_j\delta(\boldsymbol{r}-\boldsymbol{r}_j)\frac{\hbar^2\nabla_j^2}{2m}|\Psi'\rangle\\&+\frac{\omega_p^2}{4\pi}\nabla\left\{\Theta(a-r)\nabla\int d^3r_1\frac{1}{|\boldsymbol{r}-\boldsymbol{r}_1|}\delta\rho(\boldsymbol{r}_1,t)\right\}\\&+\frac{en_e}{m}\nabla\{\Theta(a-r)\nabla\varphi_1(\boldsymbol{r}_1,t)\}.\end{aligned} \tag{12}$$

According to the Thomas–Fermi approximation[19] the RPA averaged kinetic energy can be represented as follows:

$$\begin{aligned}&\langle\Psi'|-\sum_j\delta(\boldsymbol{r}-\boldsymbol{r}_j)\frac{\hbar^2\nabla_j^2}{2m}|\Psi'\rangle\\&\simeq\frac{3}{5}(3\pi^2)^{2/3}\frac{\hbar^2}{2m}\rho^{5/3}(\boldsymbol{r},t)=\frac{3}{5}(3\pi^2)^{2/3}\frac{\hbar^2}{2m}n_e^{5/3}\Theta(a-r)\\&\times\left[1+\frac{5}{3}\frac{\delta\rho(\boldsymbol{r},t)}{n_e}+\cdots\right].\end{aligned} \tag{13}$$

Taking then into account the above approximation and that $\nabla\Theta(a-r)=-\frac{\boldsymbol{r}}{r}\delta(a-r)$ as well as that $\varphi_1(\boldsymbol{R},\boldsymbol{r},t)=-\boldsymbol{r}\cdot\boldsymbol{E}(\boldsymbol{R},t)$, one can rewrite Eq. (12) in the following manner:

$$\begin{aligned}\frac{\partial^2\delta\rho(\boldsymbol{r})}{\partial t^2}=&\left[\frac{2}{3}\frac{\epsilon_F}{m}\nabla^2\delta\rho(\boldsymbol{r},t)-\omega_p^2\delta\rho(\boldsymbol{r},t)\right]\Theta(a-r)\\&-\frac{2}{3m}\nabla\left\{\left[\frac{3}{5}\epsilon_F n_e+\epsilon_F\delta\rho(\boldsymbol{r},t)\right]\frac{\boldsymbol{r}}{r}\delta(a-r)\right\}\\&-\left[\frac{2}{3}\frac{\epsilon_F}{m}\frac{\boldsymbol{r}}{r}\nabla\,\delta\rho(\boldsymbol{r},t)\right.\\&+\frac{\omega_p^2}{4\pi}\frac{\boldsymbol{r}}{r}\nabla\int d^3r_1\frac{1}{|\boldsymbol{r}-\boldsymbol{r}_1|}\delta\rho(\boldsymbol{r}_1,t)\\&\left.+\frac{en_e}{m}\frac{\boldsymbol{r}}{r}\cdot\boldsymbol{E}(\boldsymbol{R},t)\right]\delta(a-r).\end{aligned} \tag{14}$$

In the above formula ω_p is the bulk plasmon frequency, and $\omega_p^2=(4\pi n_e e^2/m)$. The solution of Eq. (14) can be decomposed into two parts that are related to the partial domains,

$$\delta\rho(\boldsymbol{r},t)=\begin{cases}\delta\rho_1(\boldsymbol{r},t), & \text{for}\quad r<a,\\ \delta\rho_2(\boldsymbol{r},t), & \text{for}\quad r\geq a,\quad (r\to a+),\end{cases} \tag{15}$$

corresponding to the volume and surface excitations, respectively. These two parts of local electron density fluctuations satisfy the equations,

$$\frac{\partial^2\delta\rho_1(\boldsymbol{r},t)}{\partial t^2}=\frac{2}{3}\frac{\epsilon_F}{m}\nabla^2\delta\rho_1(\boldsymbol{r},t)-\omega_p^2\delta\rho_1(\boldsymbol{r},t) \tag{16}$$

and

$$\frac{\partial^2 \delta\rho_2(\boldsymbol{r},t)}{\partial t^2} = -\frac{2}{3m}\nabla\left\{\left[\frac{3}{5}\epsilon_F n_e + \epsilon_F \delta\rho_2(\boldsymbol{r},t)\right]\frac{\boldsymbol{r}}{r}\delta(a+\epsilon-r)\right\}$$
$$-\left\{\frac{2}{3}\frac{\epsilon_F \boldsymbol{r}}{m\ r}\nabla\ \delta\rho_2(\boldsymbol{r},t)\right.$$
$$+\frac{\omega_p^2}{4\pi}\frac{\boldsymbol{r}}{r}\nabla\int d^3r_1\frac{1}{|\boldsymbol{r}-\boldsymbol{r}_1|}[\delta\rho_1(\boldsymbol{r}_1,t)\Theta(a-r_1)$$
$$\left.+\ \delta\rho_2(\boldsymbol{r}_1,t)\Theta(r_1-a)]+\frac{en_e}{m}\frac{\boldsymbol{r}}{r}\cdot\boldsymbol{E}(\boldsymbol{R},t)\right\}$$
$$\times\delta(a+\epsilon-r). \tag{17}$$

The $\epsilon=0+$ shift in the delta argument, $\delta(a+\epsilon-r)$ is introduced, as a formal character only, to avoid the singular point position on the edge of integration (for the delta distribution).

It is clear from Eq. (16) that the volume plasmons are independent of surface plasmons. However, surface plasmons can be excited by volume plasmons due to the last but one term in Eq. (17), which expresses a coupling between surface and volume plasmons in the metallic nanosphere within the RPA semiclassical picture. This is due to the possible influence of volume charges on surface fluctuations. Oppositely, the surface charges cannot influence the interior of the nanosphere.

When the metallic sphere is embedded in a dielectric medium, the electrons on the surface interact with forces ε (dielectric susceptibility constant) times weaker compared to vacuum. To account for this, one substitutes Eq. (17) with the following one:

$$\frac{\partial^2 \delta\rho_2(\boldsymbol{r},t)}{\partial t^2} = -\frac{2}{3m}\nabla\left\{\left[\frac{3}{5}\epsilon_F n_e + \epsilon_F \delta\rho_2(\boldsymbol{r},t)\right]\frac{\boldsymbol{r}}{r}\delta(a+\epsilon-r)\right\}$$
$$-\left\{\frac{2}{3}\frac{\epsilon_F \boldsymbol{r}}{m\ r}\nabla\ \delta\rho_2(\boldsymbol{r},t)\right.$$
$$+\frac{\omega_p^2}{4\pi}\frac{\boldsymbol{r}}{r}\nabla\int d^3r_1\frac{1}{|\boldsymbol{r}-\boldsymbol{r}_1|}\left[\delta\rho_1(\boldsymbol{r}_1,t)\Theta(a-r_1)\right.$$
$$\left.\left.+\frac{1}{\varepsilon}\delta\rho_2(\boldsymbol{r}_1,t)\Theta(r_1-a)\right]+\frac{en_e}{m}\frac{\boldsymbol{r}}{r}\cdot\boldsymbol{E}(\boldsymbol{R},t)\right\}\delta(a$$
$$+\epsilon-r). \tag{18}$$

Simultaneously, Eq. (16) does not change, which reveals the fact that the dielectric surroundings does not influence volume plasmon modes, oppositely to surface modes. One can expect that influence of surrounding dielectric medium would cause a redshift in surface plasmon resonance, what is clear as the polarization of nearby dielectric medium induced by a fluctuating surface charge, reduces this charge due to screening, which results in turn in lowering of oscillation energy. This would be accounted for within even the classical Mie-type approach. It should be noted, however, that in Ref. 20 the stronger redshift induced by dielectric missmatch is found in comparison to the Mie-type classical estimation, for the case of nanoshells. It agrees with similar analyses for small metallic clusters.[24] In both these cases spill-out is important, resulting in a widened fuzzy domain of surface fluctuations, in opposition to a sharply defined domain of the surface modes within the semiclassical approximation. Moreover, within the semiclassical approach the inner material dielectric properties are not important [as it follows from Eq. (18)], what is no case, however, in TDLDA calculus, with fuzzy surface.[20,24] This leads to a certain overestimation of the dielectric surroundings induced redshift in the semiclassical treatment in comparison to TDLDA when the domain of surface fluctuation was wider and, therefore, more distant from screening dielectric medium polarization. This manifest itself in stronger redshift for the sharp domain of surface oscillations in semiclassical approximation, which exceeds the Mie-type classical shift and also the TDLDA redshift (as it is presented in the next subsection for surface plasmon frequencies). One can expect, however, that with growing radius of the nanosphere, when spill-out is gradually reducing, the limiting TDLDA would be convergent with the semiclassical estimation. Note that the more thorough inclusion of dielectric missmatch (as in the TDLDA method[20,24]) would have a particular significance for closely located nanospheres (in a chain or dimer) when multipolar modes would contribute to mutual coupling of the spheres. In the present paper we confine, however, our consideration to simplified dipole-type coupling only, what is justified for not too small distance of nanospheres.

Let us also assume that both volume and surface plasmon oscillations are damped with the time ratio τ_0 which can be phenomenologically accounted for via the additional term, $-(2/\tau_0)[\partial\delta\rho(\boldsymbol{r},t)/\partial t]$, to the right-hand-side of above equations. They attain the form,

$$\frac{\partial^2 \delta\rho_1(\boldsymbol{r},t)}{\partial t^2}+\frac{2}{\tau_0}\frac{\partial\delta\rho(\boldsymbol{r},t)}{\partial t}=\frac{2}{3}\frac{\epsilon_F}{m}\nabla^2\delta\widetilde{\rho}_1(\boldsymbol{r},t)-\omega_p^2\delta\rho_1(\boldsymbol{r},t) \tag{19}$$

and

$$\frac{\partial^2 \delta\rho_2(\boldsymbol{r},t)}{\partial t^2}+\frac{2}{\tau_0}\frac{\partial\delta\rho(\boldsymbol{r},t)}{\partial t}$$
$$=-\frac{2}{3m}\nabla\left\{\left[\frac{3}{5}\epsilon_F n_e + \epsilon_F \delta\rho_2(\boldsymbol{r},t)\right]\frac{\boldsymbol{r}}{r}\delta(a+\epsilon-r)\right\}$$
$$-\left\{\frac{2}{3}\frac{\epsilon_F \boldsymbol{r}}{m\ r}\nabla\ \delta\widetilde{\rho}_2(\boldsymbol{r},t)\right.$$
$$+\frac{\omega_p^2}{4\pi}\frac{\boldsymbol{r}}{r}\nabla\int d^3r_1\frac{1}{|\boldsymbol{r}-\boldsymbol{r}_1|}\left[\delta\rho_1(\boldsymbol{r}_1,t)\Theta(a-r_1)\right.$$
$$\left.\left.+\frac{1}{\varepsilon}\delta\rho_2(\boldsymbol{r}_1,t)\Theta(r_1-a)\right]+\frac{en_e}{m}\frac{\boldsymbol{r}}{r}\cdot\boldsymbol{E}(\boldsymbol{R},t)\right\}\delta(a+\epsilon-r). \tag{20}$$

From Eqs. (19) and (20) it is noticeable that the electric field homogeneous over the nanosphere does not excite volume-type plasmon oscillations but only contributes to surface plasmons.

B. Solution of RPA equations: volume and surface plasmons frequencies

Equations (19) and (20) can be solved upon imposing boundary and symmetry conditions—see Appendix. Let us write both parts of the electron fluctuation in the following manner:

$$\delta\rho_1(\boldsymbol{r},t) = n_e[f_1(r) + F(\boldsymbol{r},t)], \quad \text{for} \quad r < a,$$

$$\delta\rho_2(\boldsymbol{r},t) = n_e f_2(r) + \sigma(\Omega,t)\delta(r+\epsilon-a), \quad \text{for} \quad r \geq a, \quad (r \to a+), \tag{21}$$

and let us choose convenient initial conditions $F(\boldsymbol{r},t)|_{t=0}=0$, $\sigma(\Omega,t)|_{t=0}=0$, $[\Omega=(\theta,\psi)$—spherical angles), and $[1+f_1(r)]|_{r=a}=f_2(r)|_{r=a}$ (continuity condition), $F(\boldsymbol{r},t)|_{r\to a}=0$, $\int\rho(\boldsymbol{r},t)d^3r=N_e$ (neutrality condition).

We thus arrive at an explicit form of the solutions of Eqs. (19) and (20) (as it is described in the Appendix)

$$f_1(r) = -\frac{k_T a+1}{2}e^{-k_T(a-r)}\frac{1-e^{-2k_T r}}{k_T r}, \quad \text{for} \quad r<a,$$

$$f_2(r) = \left[k_T a - \frac{k_T a+1}{2}(1-e^{-2k_T a})\right]\frac{e^{-k_T(r-a)}}{k_T r}, \quad \text{for} \quad r \geq a, \tag{22}$$

where $k_T=\sqrt{(6\pi n_e e^2/\epsilon_F)}=\sqrt{(3\omega_p^2/v_F^2)}$. For time-dependent parts of electron fluctuations, we find,

$$F(\boldsymbol{r},t) = \sum_{l=1}^{\infty}\sum_{m=-l}^{l}\sum_{n=1}^{\infty} A_{lmn} j_l(k_{nl}r)Y_{lm}(\Omega)\sin(\omega'_{nl}t)e^{-t/\tau_0} \tag{23}$$

and

$$\sigma(\Omega,t) = \sum_{l=1}^{\infty}\sum_{m=-l}^{l} Y_{lm}(\Omega)\left[\frac{B_{lm}}{a^2}\sin(\omega'_{0l}t)e^{-t/\tau_0}(1-\delta_{1l}) + Q_{1m}(t)\delta_{1l}\right] + \sum_{l=1}^{\infty}\sum_{m=-l}^{l}\sum_{n=1}^{\infty} A_{lmn} \times \frac{(l+1)\omega_p^2}{l\omega_p^2-(2l+1)\omega_{nl}^2}Y_{lm}(\Omega)n_e \times \int_0^a dr_1 \frac{r_1^{l+2}}{a^{l+2}} j_l(k_{nl}r_1)\sin(\omega'_{nl}t)e^{-t/\tau_0}, \tag{24}$$

where $j_l(\xi)=\sqrt{(\pi/2\xi)}I_{l+1/2}(\xi)$ is the spherical Bessel function, $Y_{lm}(\Omega)$ is the spherical function, $\omega_{nl}=\omega_p\sqrt{1+(x_{nl}^2/k_T^2a^2)}$ are the frequencies of electron volume free self-oscillations (volume plasmon frequencies), x_{nl} are nodes of the Bessel function $j_l(\xi)$, $\omega_{0l}=\omega_p\sqrt{l/\varepsilon(2l+1)}$ are the frequencies of electron surface free self-oscillations (surface plasmon frequencies), and $k_{nl}=x_{nl}/a$; $\omega'=\sqrt{\omega^2-(1/\tau_0^2)}$ are the shifted frequencies for all modes due to damping. The coefficients B_{lm} and A_{lmn} are determined by the initial conditions. We assumed that $\delta\rho(\boldsymbol{r},t=0)=0$, so $B_{lm}=0$ and $A_{lmn}=0$, except for $l=1$ in the former case (of B_{lm}), which corresponds to homogeneous electric field excitation. This is described by the function $Q_{1m}(t)$ in the general solution (24). The function $Q_{1m}(t)$ satisfies the equation,

$$\frac{\partial^2 Q_{1m}(t)}{\partial t^2} + \frac{2}{\tau_0}\frac{\partial Q_{1m}(t)}{\partial t} + \omega_1^2 Q_{1m}(t) = \sqrt{\frac{4\pi}{3}}\frac{en_e}{m}\{E_z(\boldsymbol{R},t)\delta_{m0} + \sqrt{2}[E_x(\boldsymbol{R},t)\delta_{m1} + E_y(\boldsymbol{R},t)\delta_{m-1}]\}, \tag{25}$$

where $\omega_1=\omega_{01}=(\omega_p/\sqrt{3\varepsilon})$ (it is a dipole-type surface plasmon Mie frequency[13]). Only this function contributes to the dynamical response to the homogeneous electric field (for the assumed initial conditions). From the above it follows thus that the local electron density (within the RPA attitude) has the form,

$$\rho(\boldsymbol{r},t) = \rho_0(r) + \rho_1(\boldsymbol{r},t), \tag{26}$$

where the RPA equilibrium electron distribution (correcting the uniform distribution n_e),

$$\rho_0(r) = \begin{cases} n_e[1+f_1(r)], & \text{for} \quad r<a, \\ n_e f_2(r), & \text{for} \quad r \geq a, \quad r \to a+ \end{cases} \tag{27}$$

and the nonequilibrium, of surface plasmon oscillation type for the homogeneous forcing field,

$$\rho_1(\boldsymbol{r},t) = \begin{cases} 0, & \text{for} \quad r<a, \\ \sum_{m=-1}^{1} Q_{1m}(t)Y_{1m}(\Omega) & \text{for} \quad r \geq a, \quad r \to a+. \end{cases} \tag{28}$$

In general, $F(\boldsymbol{r},t)$ (volume plasmons) and $\sigma(\Omega,t)$ (surface plasmons) contribute to plasmon oscillations. However, in the case of homogeneous perturbation, only the surface $l=1$ mode is excited.

For plasmon oscillations given by Eq. (28) one can calculate the corresponding dipole,

$$\boldsymbol{D}(\boldsymbol{R},t) = e\int d^3r\boldsymbol{r}\rho(\boldsymbol{r},t) = \frac{4\pi}{3}e\boldsymbol{q}(\boldsymbol{R},t)a^3, \tag{29}$$

where $Q_{11}(\boldsymbol{R},t)=\sqrt{(8\pi/3)}q_x(\boldsymbol{R},t)$, $Q_{1-1}(\boldsymbol{R},t)=\sqrt{(8\pi/3)}q_y(\boldsymbol{R},t)$, $Q_{10}(\boldsymbol{R},t)=\sqrt{(4\pi/3)}q_x(\boldsymbol{R},t)$, and $\boldsymbol{q}(\boldsymbol{R},t)$ satisfies the equation [see Eq. (25)],

$$\left[\frac{\partial^2}{\partial t^2} + \frac{2}{\tau_0}\frac{\partial}{\partial t} + \omega_1^2\right]\boldsymbol{q}(\boldsymbol{R},t) = \frac{en_e}{m}\boldsymbol{E}(\boldsymbol{R},t). \tag{30}$$

III. LORENTZ FRICTION FOR NANOSPHERE PLASMONS

Considering the nanosphere plasmons induced by the homogeneous electric field, as described in the above paragraph, one can note that these plasmons are themselves a source of electromagnetic (e-m) radiation. This radiation takes away the energy of plasmons resulting in their damping, which can be described as the Lorentz friction.[25] This e-m wave emission causes electron friction which can be described as an additional electric field,[25]

$$\boldsymbol{E}_L = \frac{2}{3\varepsilon v^2}\frac{\partial^3 \boldsymbol{D}(t)}{\partial t^3}, \tag{31}$$

where $v=(c/\sqrt{\varepsilon})$ is the light velocity in the dielectric medium, and $\boldsymbol{D}(t)$ the dipole of the nanosphere. According to Eq. (29) we arrive at the following:

$$\boldsymbol{E}_L = \frac{2e}{3\varepsilon v^2}\frac{4\pi}{3}a^3\frac{\partial^3 \boldsymbol{q}(t)}{\partial t^3}. \tag{32}$$

Substituting this into Eq. (30), we get,

$$\left[\frac{\partial^2}{\partial t^2}+\frac{2}{\tau_0}\frac{\partial}{\partial t}+\omega_1^2\right]\boldsymbol{q}(\boldsymbol{R},t) = \frac{en_e}{m}\boldsymbol{E}(\boldsymbol{R},t)+\frac{2}{3\omega_1}\left(\frac{\omega_1 a}{v}\right)^3\frac{\partial^3 \boldsymbol{q}(\boldsymbol{R},t)}{\partial t^3}. \tag{33}$$

If one rewrites the above equation (for $\boldsymbol{E}=0$) in the form,

$$\left[\frac{\partial^2}{\partial t^2}+\omega_1^2\right]\boldsymbol{q}(\boldsymbol{R},t) = \frac{\partial}{\partial t}\left[-\frac{2}{\tau_0}\boldsymbol{q}(\boldsymbol{R},t)+\frac{2}{3\omega_1}\left(\frac{\omega_1 a}{v}\right)^3\frac{\partial^2 \boldsymbol{q}(\boldsymbol{R},t)}{\partial t^2}\right], \tag{34}$$

thus, one notes that the zeroth order approximation (neglecting attenuation) corresponds to the equation,

$$\left[\frac{\partial^2}{\partial t^2}+\omega_1^2\right]\boldsymbol{q}(\boldsymbol{R},t)=0. \tag{35}$$

In order to solve Eq. (34) in the next step of perturbation, one can substitute, in the right-hand-side of this equation, $\partial^2\boldsymbol{q}(t)/\partial t^2$ by $-\omega_1^2\boldsymbol{q}(t)$ [according to Eq. (35)].

Therefore, if one assumes the above estimation, $(\partial^3\boldsymbol{q}(t)/\partial t^3)\simeq-\omega_1^2(\partial\boldsymbol{q}(t)/\partial t)$, one can include the Lorentz friction in a renormalized damping term,

$$\left[\frac{\partial^2}{\partial t^2}+\frac{2}{\tau}\frac{\partial}{\partial t}+\omega_1^2\right]\boldsymbol{q}(\boldsymbol{R},t)=\frac{en_e}{m}\boldsymbol{E}(\boldsymbol{R},t), \tag{36}$$

where

TABLE I. a_0—nanosphere radius corresponding to minimal damping.

Refraction rate of the surrounding medium, n_0	Au, a_0 (nm)	Ag, a_0 (nm)	Cu, a_0 (nm)
(Air) 1	8.8	8.44	8.46
(Water) 1.4	9.14	9.18	9.20
(Colloidal solution) 2	9.99	10.04	10.04

$$\frac{1}{\tau}=\frac{1}{\tau_0}+\frac{\omega_1}{3}\left(\frac{\omega_1 a}{v}\right)^3\simeq\frac{v_F}{2\lambda_B}+\frac{Cv_F}{2a}+\frac{\omega_1}{3}\left(\frac{\omega_1 a}{v}\right)^3, \tag{37}$$

where we used for $(1/\tau_0)\simeq(v_F/2\lambda_B)+(Cv_F/2a)$, ($\lambda_B$ is the free path in bulk, v_F is the Fermi velocity, and $C\simeq1$ is a constant),[26–28] which corresponds to inclusion of plasmon damping due to electron scattering on other electrons and on the nanoparticle boundary. Renormalized damping causes a change in the shift in self-frequencies of free surface plasmons, $\omega_1'=\sqrt{\omega_1^2-(1/\tau^2)}$.

Using Eq. (37) one can determine the radius a_0 that corresponds to minimal damping,

$$a_0=\frac{\sqrt{3}}{\omega_p}(v_F c^3\sqrt{\varepsilon}/2)^{1/4}. \tag{38}$$

For nanoparticles of gold, silver and copper in air, in water, and in a colloidal solution, one can find $a_0\leq10$ nm (see Table I), which corresponds to the experimental data.[29,30] For $a>a_0$ damping increases due to Lorentz friction (proportional to a^3) but for $a<a_0$, the damping due to electron scattering dominates and grows with lowering a [as $\sim(1/a)$, see Fig. 1], which agrees with experimental observations.[26,29]

Surface plasmon oscillations cause attenuation of the incident e-m radiation, with maximum of attenuation at the resonant frequency[22] $\omega_1'=\sqrt{\omega_1^2-(1/\tau^2)}$. This frequency diminishes with the rise of a, for $a>a_0$ according to Eq. (37), which agrees with experimental observations for Au and Ag presented in Fig. 2, and Table II (Au) and Table III (Ag).

Note that the Lorentz friction, being of the third order with respect to time-retardation shift,[25] includes the retardation effects via plasmon damping induced by irradiation.[31] The other channel of plasmon damping corresponds to non-

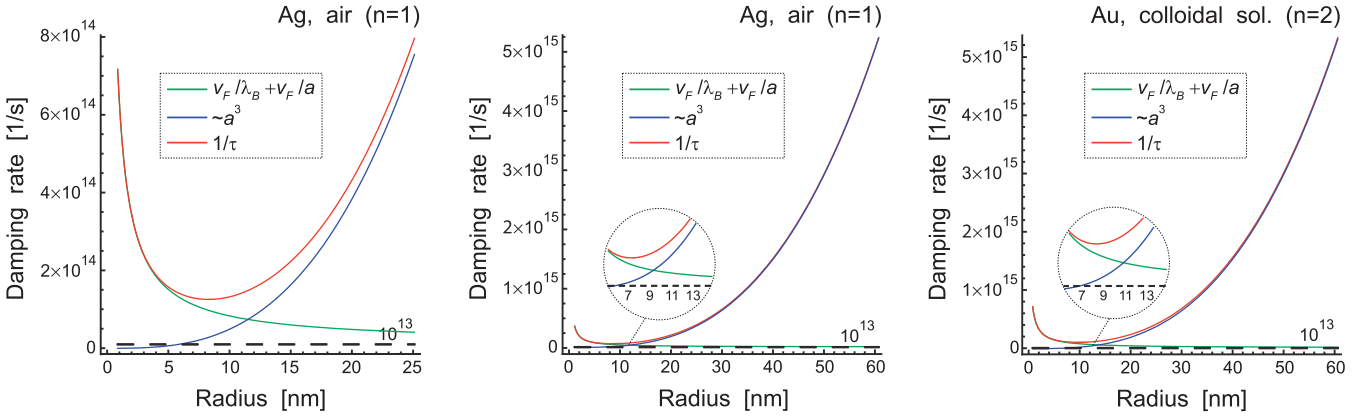

FIG. 1. (Color) Effective damping ratios for surface plasmon oscillations for Ag in air (left and middle) and Au colloidal solutions (right) from Eq. (38), respectively. The red curve represents the sum of both terms, the green is the term $\sim(1/a)$, and the blue is the term $\sim a^3$; the minimum corresponds to the minimal damping for radius a_0 from Eq. (39).

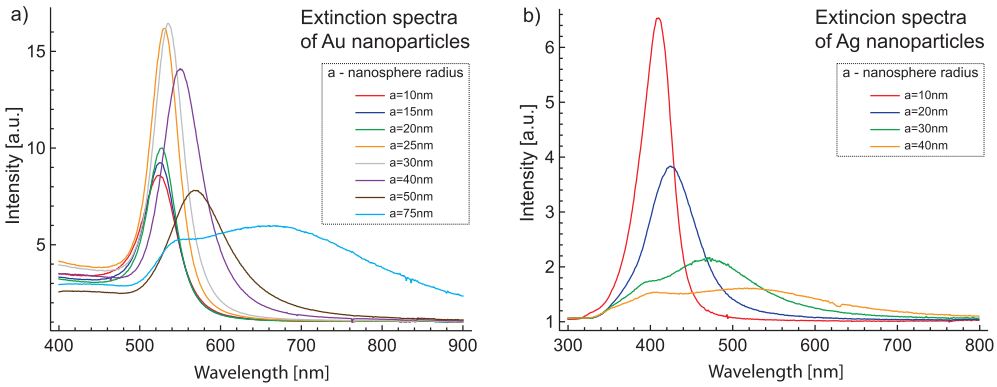

FIG. 2. (Color) Extinction spectra for nanospheres of Au (a) and Ag (b) in colloidal water solution for various sphere radii; Lorentzian shapes correspond to light attenuation due to surface plasmons exciting in nanospheres; for large radii (~75 nm for Au and ~30–40 nm for Ag) the second attenuation peak appears corresponding possibly to volume mode excited at nonexact dipole approximation regime.

local effects including scattering on the nanoparticle surface.[32] We have demonstrated that the retardation and the nonlocal effects lead to opposite, redshift and blueshift in the resonance frequency, similarly as it was indicated in Ref. 31.

IV. UNDAMPED SURFACE PLASMON COLLECTIVE EXCITATION ALONG A CHAIN OF METALLIC NANOSPHERES

Let us consider a linear chain of metallic nanospheres with radii a in a dielectric medium with dielectric constant ε. We assume that spheres are located along the z-axis direction equidistantly with the separation of the sphere centers $d > 2a$.[26,33] At time $t=0$ we assume the excitation of plasmon oscillations via a Dirac delta, $\sim\delta(t)$, shaped signal of electric field. Taking into account the mutual interaction of the induced surface plasmons on the spheres via the radiation of dipole oscillations, we aim to determine the stationary state of the whole infinite chain. For a separation d much shorter than the wavelength λ of the e-m wave corresponding to surface plasmon self-frequency in a single nanosphere, the dipole-type plasmon radiation can be treated within the near-field regime, at least for nearest neighboring spheres. In the near-field region $a < R_0 < \lambda$, the radiation of the dipole $\boldsymbol{D}(t)$ is not a planar wave (as it is for far-field region, $R_0 \gg \lambda$) but is of only a retarded electric field (without a magnetic field)[25]

$$\boldsymbol{E}(\boldsymbol{R},\boldsymbol{R}_0,t) = \frac{1}{\varepsilon R_0^3}\left\{3\boldsymbol{n}\left[\boldsymbol{n}\cdot\boldsymbol{D}\left(\boldsymbol{R},t-\frac{R_0}{v}\right)\right] - \boldsymbol{D}\left(\boldsymbol{R},t-\frac{R_0}{v}\right)\right\}, \tag{39}$$

$\boldsymbol{R}$ is the position of the sphere (center) irradiating e-m energy due to its dipole surface plasmon oscillations, $\boldsymbol{R}_0$ is the position of another sphere (center), with respect to the center of the former one, where the field $\boldsymbol{E}(\boldsymbol{R},\boldsymbol{R}_0,t)$ is given by the above formula, $R_0 < \lambda$, $\boldsymbol{n}=\boldsymbol{R}_0/R_0$, and $v=c/\sqrt{\varepsilon}=c/n_0$.

When both vectors $\boldsymbol{R}$ and $\boldsymbol{R}_0$ are along the z-axis (the linear chain) the above equation can be resolved as,

$$E_\alpha(\boldsymbol{R},\boldsymbol{R}_0,t) = \frac{\sigma_\alpha}{\varepsilon R_0^3} D_\alpha\left(\boldsymbol{R},t-\frac{R_0}{v}\right), \tag{40}$$

where $\alpha=(x,y,z)$, $\sigma_x=\sigma_y=-1$, and $\sigma_z=2$. Assuming that the z-axis origin coincides with the center of one sphere in the chain, for the lth sphere located in the point $\boldsymbol{R}_l=(0,0,ld)$, an electric field caused by neighboring spheres, $\boldsymbol{E}(\boldsymbol{R}_m,\boldsymbol{R}_{ml},t)$, and the Lorentz friction force caused by self-radiation, $\boldsymbol{E}_L(\boldsymbol{R}_l,t)$, have to be accounted for. By virtue of Eq. (30) the equation for the surface plasmon oscillation of the lth sphere is,

$$\left[\frac{\partial^2}{\partial t^2}+\frac{2}{\tau_0}\frac{\partial}{\partial t}+\omega_1^2\right]\boldsymbol{q}(\boldsymbol{R}_l,t) = \frac{en_e}{m}\sum_{m=-\infty,m\neq l,R_{ml}<\lambda}^{m=\infty}\boldsymbol{E}(\boldsymbol{R}_m,\boldsymbol{R}_{ml},t) + \frac{en_e}{m}\boldsymbol{E}_L(\boldsymbol{R}_l,t), \tag{41}$$

provided that the dipole field of the mth sphere can be treated as homogeneous over the lth sphere and the sum over m is confined by the distance of the mth sphere from the lth sphere not exceeding the near-field range (~λ). In the case of the equidistant chain, $R_l=ld$ and $R_{ml}=|l-m|d$, and using Eqs. (40), (29), and (32), one can rewrite Eq. (41) in the form,

$$\left[\frac{\partial^2}{\partial t^2}+\frac{2}{\tau_0}\frac{\partial}{\partial t}-\frac{2}{3\omega_1}\left(\frac{\omega_1 a}{v}\right)^3\frac{\partial^3}{\partial t^3}+\omega_1^2\right]q_\alpha(ld,t) = \sigma_\alpha\omega_1^2\frac{a^3}{d^3}\sum_{m=-\infty,m\neq l,|l-m|d<\lambda}^{m=\infty}\frac{q_\alpha\left(md,t-\frac{d}{v}|l-m|\right)}{|l-m|^3}, \tag{42}$$

where $\alpha=x,y$, which describe the transversal plasmon modes

TABLE II. Resonant frequency for e-m wave attenuation in Au nanospheres.

Radius of nanospheres (nm)	10	15	20	25	30	40	50
$\hbar\omega_1'$ (experiment) (eV)	2.371	2.362	2.357	2.340	2.316	2.248	2.172
$\hbar\omega_1'$ (theory) (eV), $n_0=1.4$	3.721	3.720	3.716	2.702	3.666	3.415	2.374
$\hbar\omega_1'$ (theory) (eV), $n_0=2$	2.604	2.603	2.600	2.590	2.565	2.388	1.656

TABLE III. Resonant frequency for e-m wave attenuation in Ag nanospheres.

Radius of nanospheres (nm)	10	20	30	40
$\hbar\omega_1'$ (experiment) (eV)	3.024	2.911	2.633	2.385
$\hbar\omega_1'$ (theory) (eV), $n_0=1.4$	3.707	3.702	3.654	3.410
$\hbar\omega_1'$ (theory) (eV), $n_0=2$	2.595	2.591	2.557	2.384

and $\alpha=z$, which describes the longitudinal mode; $\omega_1^2=(\omega_p^2/3\varepsilon)=(4\pi n_e e^2/3\varepsilon m)$ and $v=(c/\sqrt{\varepsilon})$. The above equation coincides with the appropriate one from Refs. 26 and 33, if one assumes that $(4\pi/3)a^3n_e=N=1$ and neglects the retardation of the field.

Taking into account the periodicity of the infinite chain, one can consider the solution of the above equation in the form,

$$q_\alpha(ld,t)=\tilde{q}_\alpha(k,t)e^{-ikld}. \tag{43}$$

The right-hand-side term in Eq. (42) attains the form,

$$\begin{aligned}
&\sum_{m=-\infty,m\neq l}^{m=\infty}\frac{q_\alpha\left(md,t-\frac{d}{v}|l-m|\right)}{|l-m|^3}\\
&=\sum_{m=-\infty}^{l-1}\frac{q_\alpha\left(md,t-\frac{d}{v}|l-m|\right)}{|l-m|^3}\\
&\quad+\sum_{m=l+1}^{m=\infty}\frac{q_\alpha\left(md,t-\frac{d}{v}|l-m|\right)}{|l-m|^3}\\
&=2e^{-ikld}\sum_{m=1}^{\infty}\frac{\cos(mkd)}{m^3}\tilde{q}_\alpha(k,t-md/v).
\end{aligned}$$

Thus, the Eq. (42) can be written as follows:

$$\begin{aligned}
&\left[\frac{\partial^2}{\partial t^2}+\frac{2}{\tau_0}\frac{\partial}{\partial t}-\frac{2}{3\omega_1}\left(\frac{\omega_1 a}{v}\right)^3\frac{\partial^3}{\partial t^3}+\omega_1^2\right]\tilde{q}_\alpha(k,t)\\
&=\sigma_\alpha\omega_1^2\frac{a^3}{d^3}2\sum_{m=1,md<\lambda}^{\infty}\frac{\cos(mkd)}{m^3}\tilde{q}_\alpha(k,t-md/v).
\end{aligned}\tag{44}$$

This equation is linear and, therefore, we look for the solutions of the shape: $\tilde{q}_\alpha(k,t)=\tilde{Q}_\alpha(k)e^{i\omega_\alpha t}$, and we arrive at the condition,

$$-\omega_\alpha^2+\frac{2i\omega_\alpha}{\tau_\alpha(\omega_\alpha)}+\tilde{\omega}_\alpha^2(\omega_\alpha)=0, \tag{45}$$

where,

$$\tilde{\omega}_\alpha^2(\omega_\alpha)=\omega_1^2\left[1-\frac{2\sigma_\alpha a^3}{d^3}\sum_{m=1,md<\lambda}^{\infty}\frac{\cos(mkd)}{m^3}\cos\left(\frac{\omega_\alpha md}{v}\right)\right] \tag{46}$$

and

$$\begin{aligned}
\frac{1}{\tau_\alpha(\omega_\alpha)}&=\frac{1}{\tau_0}+\frac{\omega_1^2 a}{3v}\left(\frac{\omega_\alpha a}{v}\right)^2\\
&\quad+\sigma_\alpha\omega_1^2\frac{a^3}{d^3}\sum_{m=1,md<\lambda}^{\infty}\frac{\cos(mkd)}{m^3}\frac{\sin\left(\frac{\omega_\alpha md}{v}\right)}{\omega_\alpha}.
\end{aligned}\tag{47}$$

If we confine the sum in Eq. (46) to $m=1$ (the nearest neighbor approximation), we get,

$$\tilde{\omega}_\alpha^2(\omega_\alpha)\simeq\omega_1^2\left[1-\frac{2\sigma_\alpha a^3}{d^3}\cos(kd)\cos\left(\frac{\omega_\alpha d}{v}\right)\right] \tag{48}$$

and from Eq. (47),

$$\frac{1}{\tau_\alpha(\omega_\alpha)}=\frac{1}{\tau_0}+\frac{\omega_1^2 a^3}{4vd^2}\left[\left(\frac{\omega_\alpha d}{v}\right)^2-(kd-\pi)^2+\frac{\pi^2}{3}\right],\quad\text{for}\quad\alpha=x,y \tag{49}$$

and

$$\frac{1}{\tau_z(\omega_z)}=\frac{1}{\tau_0}+\frac{\omega_1^2 a^3}{2vd^2}\left[\left(\frac{\omega_z d}{v}\right)^2+(kd-\pi)^2-\frac{\pi^2}{3}\right],\quad\text{for}\quad\alpha=z. \tag{50}$$

In the derivation of the two above formulae the following summation was performed:[34]

$$\begin{aligned}
&\frac{1}{\omega_\alpha}\sum_{m=1}^{\infty}\frac{\cos(mkd)}{m^3}\sin\left(\frac{\omega_\alpha md}{v}\right)\\
&=\frac{1}{2\omega_\alpha}\sum_{m=1}^{\infty}\frac{1}{m^3}[\sin(kmd+\omega_\alpha md/v)-\sin(kmd-\omega_\alpha md/v)]\\
&=\frac{d}{v}\left[\frac{\pi^2}{6}-\frac{\pi}{2}kd+\frac{k^2d^2}{4}+\frac{\omega_\alpha^2d^2}{2v^2}\right].
\end{aligned}$$

Because the terms in the sum drop quickly to zero, the above formula approximates well the sum with limitation $md<\lambda$.

Assuming now, $\omega_\alpha=\omega_\alpha'+i\omega_\alpha''$, the Eq. (45) gives the dependence of ω_α' and ω_α'' on k. The general solution of Eq. (42) attains the form,

$$q_\alpha(ld,t)=\sum_{n=1}^{N_s}\tilde{Q}_\alpha(k_n)e^{i(\omega_\alpha'(k_n)t-k_nld)-\omega_\alpha''(k_n)t}, \tag{51}$$

where $k_n=(2\pi n/N_s d)$, $L=N_s d$ is the assumed length of the chain with N_s spheres, when periodic (Born–Karman-type) boundary conditions are imposed. The components of Eq. (51) describe monochromatic waves with wavelength $\lambda_n=(2\pi/k_n)=(L/n)$, which are analogous to planar waves in crystals, when damping is not big, i.e., when $\omega_\alpha''\ll\omega_\alpha'$. Provided with this inequality, one can approximate: for the transversal modes $(\alpha=x,y)$,

$$(\omega_\alpha')^2=\tilde{\omega}_\alpha^2=\omega_1^2\left[1+\frac{2a^3}{d^3}\cos(kd)\cos(\omega_\alpha' d/v)\right], \tag{52}$$

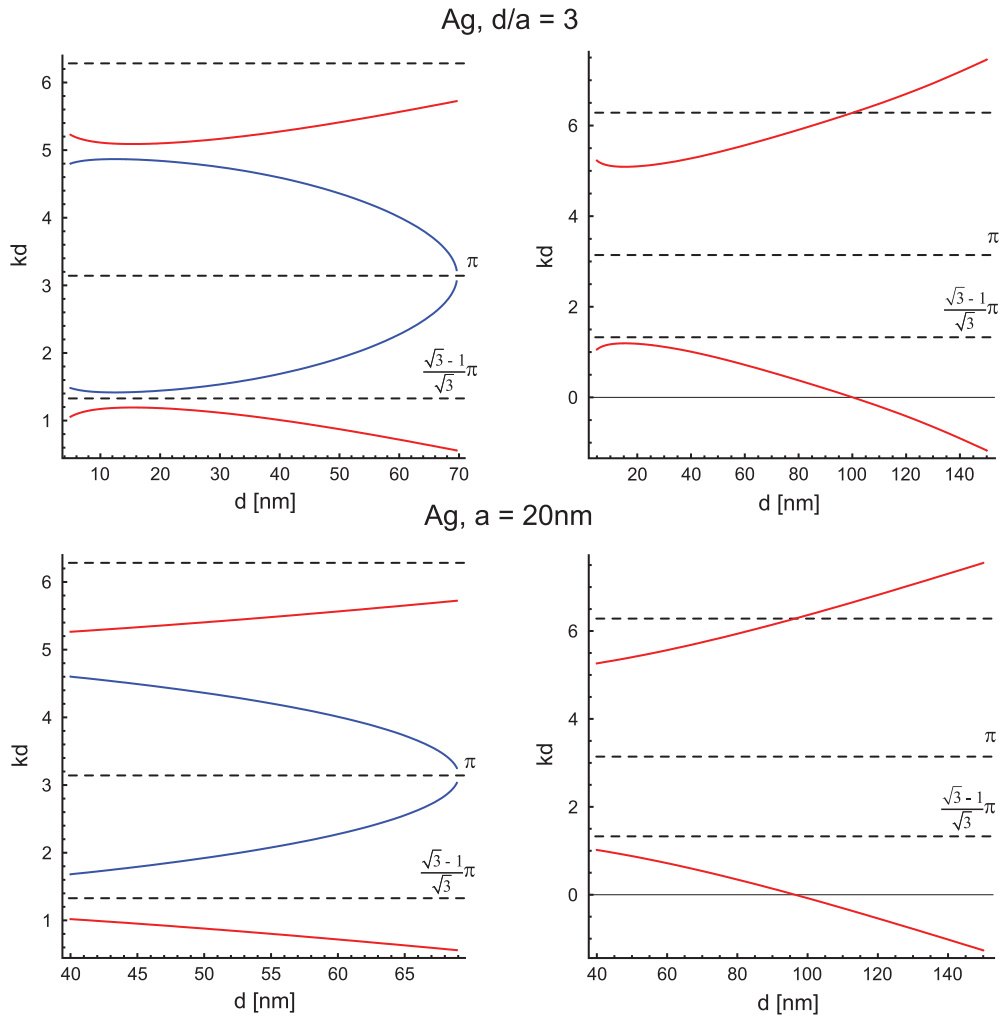

FIG. 3. (Color) Wave vector kd for undamped surface plasmon propagation along the metallic nanosphere chain vs sphere separation d at (top) constant $d/a=3$, with a the sphere radius and (bottom) for $a=20$ nm for Ag sphere chains, respectively; transversal modes are shown in red while longitudinal modes are shown in blue.

$$\omega_\alpha'' = \frac{1}{\tau_\alpha} = \frac{1}{\tau_0} + \frac{\omega_1^2 a^3}{4vd^2}\left[\left(\frac{\omega_\alpha' d}{v}\right)^2 - (kd-\pi)^2 + \frac{\pi^2}{3}\right], \quad (53)$$

and for the longitudinal mode ($\alpha=z$),

$$(\omega_z')^2 = \tilde{\omega}_z^2 = \omega_1^2\left[1 - \frac{4a^3}{d^3}\cos(kd)\cos(\omega_z' d/v)\right], \quad (54)$$

$$\omega_z'' = \frac{1}{\tau_z} = \frac{1}{\tau_0} + \frac{\omega_1^2 a^3}{2vd^2}\left[\left(\frac{\omega_\alpha' d}{v}\right)^2 + (kd-\pi)^2 - \frac{\pi^2}{3}\right]. \quad (55)$$

From Eqs. (53) and (55) it follows that ω_α'' can change its sign. In the case of $\omega_\alpha''<0$ the oscillations are destabilized, which could be avoided by inclusions of some nonlinear terms neglected in the expression for the Lorentz friction, which in more accurate form[25] includes also a small nonlinear term with respect to D, aside from the term with $\partial^3 D/\partial t^3$. Including this will result in damping of too highly rising oscillations and will lead to stable oscillation amplitude. Due to this stabilization caused by nonlinear effects, undamped wave modes of dipole oscillations will propagate in the chain in the region of parameters where $\omega_\alpha'' \leq 0$ (and with fixed amplitude accommodated by the nonlinear term). The condition $\omega_\alpha''=(1/\tau_\alpha)=0$, for critical parameters, resolves into,

$$\left(\frac{\omega_\alpha d}{v}\right)^2 = (kd-\pi)^2 - \frac{\pi^2}{3} - \frac{4vd^2}{\tau_0\omega_1^2 a^3}, \quad (56)$$

for $\alpha=(x,y)$ and for $\alpha=z$,

$$\left(\frac{\omega_z d}{v}\right)^2 = -(kd-\pi)^2 + \frac{\pi^2}{3} - \frac{2vd^2}{\tau_0\omega_1^2 a^3}. \quad (57)$$

$(\omega_\alpha d/v)$ obtained from the above equations leads to determination of the dependence of wave vector k with respect to parameters d and a, via Eqs. (52)–(55). Solutions for these equations, found numerically for the chain of Ag nanospheres, are depicted in Fig. 3.

Undamped plasmon waves in the chain appear if $d < d_{\max}$ and have $k=\pi/d$, $d_{\max}=98.5(68.8)$ nm for transversal(longitudinal) modes. For example, for Ag spheres with the radius $a=20$ nm and the separation $d=60$ nm, undamped transversal modes appear for $0\leq kd\leq \pi/4$ or $3\pi/4\leq kd\leq 2\pi$ and an undamped longitudal mode for $3\pi/4\leq kd\leq 5\pi/4$.

Let us underline that the determined undamped plasmon oscillation wave modes would explain similar, numerically

observed behavior.[35–37] Within that numerical analysis two types of collective surface plasmons with distinct propagation along the nanosphere chain were identified, and called as quasistatic (ordinary) and nonquasistatic (extraordinary) surface plasmon modes. The quasistatic modes were damped while nonquasistatic ones were undamped (and additionally, the latter turn out to be relatively robust against the disorder in the chain).[35] One can associate these observations with undamped collective plasmon modes with the negative imaginary part of the frequency, accessible in the described above regions of the chain parameters and the wave vector values (stabilized by nonlinear terms of Lorentz friction at a certain amplitude), which are, however, accompanied by ordinary damped modes with the positive imaginary frequency part.

V. CONCLUSIONS

In the present paper we analyzed plasmons in large metallic nanospheres induced by a homogeneous time-dependent electric field. Within an all-analytical RPA quasiclassical approach, the volume and surface plasmons are described. It was verified that only dipole-type of surface plasmons can be induced by a homogeneous field (while none of volume modes). An irradiation of energy by plasmon oscillations is described within the Lorentz friction effect. Its scaling with the nanosphere dimension leads to a sphere radius dependent shift in resonant frequency, similarly as observed in experiments, for nonsmall nanospheres (with radii 10–80 nm). This description of surface dipole-type plasmon oscillations in a single nanosphere is applied to the analysis of collective oscillations in linear chains of metallic nanospheres. The wave-type collective plasmon oscillations in the chain are also considered. The undamped region of wave propagation through the chain is found for a certain sphere separation in the chain with the corresponding wavelength of plasmon waves. This phenomenon confirms similar behavior observed by numerical simulations.[35]

ACKNOWLEDGMENTS

Supported by the Polish KBN Project No. N N202 260734 and the FNP Fellowship Start (W.J.), as well as DFG under Grant No. SCHA 1576/1-1 (D. Z. Hu and D.S.).

APPENDIX: ANALYTICAL SOLUTION OF PLASMON EQUATIONS FOR THE NANOSPHERE

Let us solve first the Eq. (19), assuming a solution in the form,

$$\delta\rho_1(\boldsymbol{r},t) = n_e[f_1(r) + F(\boldsymbol{r},t)], \quad \text{for} \quad r < a. \tag{A1}$$

Equation (19) resolves thus into,

$$\nabla^2 f_1(r) - k_T^2 f_1(r) = 0,$$

$$\frac{\partial^2 F(\boldsymbol{r},t)}{\partial t^2} + \frac{2}{\tau_0}\frac{\partial F(\boldsymbol{r},t)}{\partial t} = \frac{v_F^2}{3}\nabla^2 F(\boldsymbol{r},t) - \omega_p^2 F(\boldsymbol{r},t). \tag{A2}$$

The solution for function $f_1(r)$ (nonsingular at $r=0$) thus has the form,

$$f_1(r) = \alpha\frac{e^{-k_T a}}{k_T r}(e^{-k_T r} - e^{k_T r}), \tag{A3}$$

where α is a constant, $k_T = \sqrt{6\pi n_e e^2/\epsilon_F} = \sqrt{3\omega_p^2/v_F^2}$ (k_T is the inverse Thomas–Fermi radius), $\omega_p = \sqrt{4\pi n_e e^2/m}$; (bulk plasmon frequency).

Since we assume $F(\boldsymbol{r},0)=0$, then for function $F(\boldsymbol{r},t)$ the solution can be taken as,

$$F(\boldsymbol{r},t) = F_\omega(\boldsymbol{r})\sin(\omega' t)e^{-\tau_0 t}, \tag{A4}$$

where $\omega' = \sqrt{\omega^2 + 1/\tau_0^2}$. $F_\omega(\boldsymbol{r})$ satisfies the equation (Helmholtz equation),

$$\nabla^2 F_\omega(\boldsymbol{r}) + k^2 F_\omega(\boldsymbol{r}) = 0, \tag{A5}$$

with $k^2 = (\omega^2 - \omega_p^2/v_F^2/3)$. A solution of the above equation, nonsingular at $r=0$, is as follows,

$$F_\omega(\boldsymbol{r}) = A j_l(kr) Y_{lm}(\Omega), \tag{A6}$$

where A is a constant, $j_l(\xi) = \sqrt{\pi/(2\xi)} I_{l+1/2}(\xi)$ is the spherical Bessel function [$I_n(\xi)$ is the Bessel function of the first order], $Y_{lm}(\Omega)$ is the spherical function (Ω is the spherical angle). Owing to the quasiclassical boundary condition, $F(\boldsymbol{r},t)|_{r\to a}=0$, one has to demand $j_l(ka)=0$, which leads to the discrete values of $k=k_{nl}=x_{nl}/a$, (where x_{nl}, $n=1,2,3,\ldots$, are nodes of j_l), and next to the discretisation of self-frequencies ω,

$$\omega_{nl}^2 = \omega_p^2\left(1 + \frac{x_{nl}^2}{k_T^2 a^2}\right). \tag{A7}$$

The general solution for $F(\boldsymbol{r},t)$ thus has the form,

$$F(\boldsymbol{r},t) = \sum_{l=0}^{\infty}\sum_{m=-l}^{l}\sum_{n=1}^{\infty} A_{lmn} j_l(k_{nl} r) Y_{lm}(\Omega)\sin(\omega'_{nl} t)e^{-\tau_0 t}. \tag{A8}$$

A solution of Eq. (20) we represent as,

$$\delta\rho_2(\boldsymbol{r},t) = n_e f_2(r) + \sigma(\Omega,t)\delta(r+\epsilon-a), \quad \text{for} \quad r \geq a, \quad (r \to a+, i.e., \epsilon = 0+). \tag{A9}$$

The neutrality condition, $\int \rho(\boldsymbol{r},t)d^3r = N_e$, with $\delta\rho_2(\boldsymbol{r},t) = \sigma(\omega,t)\delta(a+\epsilon-r) + n_e f_2(r)$, ($\epsilon\to 0$), can be rewritten as follows: $-\int_0^a dr r^2 f_1(r) = \int_a^\infty dr r^2 f_2(r)$, $\int_0^a d^3 r F(\boldsymbol{r},t) = 0$, and $\int d\Omega\sigma(\Omega,t) = 0$. Taking into account also the continuity condition on the spherical particle surface, $1 + f_1(a) = f_2(a)$, one can obtain: $f_2(r) = \beta e^{-k_T(r-a)}/(k_T r)$. It is possible to fit α [see Eq. (A3)] and β constants: $\alpha = (k_T a + 1/2)$ and $\beta = k_T a - (k_T a + 1/2)(1 - e^{-2k_T a})$—which gives Eqs. (22).

From the condition $\int_0^a d^3 r F(\boldsymbol{r},t) = 0$ and from Eq. (A8) it follows that $A_{00n} = 0$, (because of $\int d\Omega Y_{lm}(\omega) = 4\pi\delta_{l0}\delta_{m0}$).

To remove the Dirac delta functions we integrate both sides of the Eq. (20) with respect to the radius ($\int_0^\infty r^2 dr \ldots$) and then we take the limit to the sphere surface, $\epsilon\to 0$. This results in the following equation for surface plasmons:

$$\frac{\partial^2\sigma(\Omega,t)}{\partial t^2}+\frac{2}{\tau_0}\frac{\partial\sigma(\Omega,t)}{\partial t}=-\sum_{l=0}^{\infty}\sum_{m=-l}^{l}\omega_{0l}^2Y_{lm}(\Omega)\int d\Omega_1\sigma(\Omega_1,t)Y_{lm}^*(\Omega_1)$$
$$+\omega_p^2n_e\sum_{l=0}^{\infty}\sum_{m=-l}^{l}\sum_{n=1}^{\infty}A_{lmn}\frac{l+1}{2l+1}Y_{lm}(\Omega)\int_0^a dr_1\frac{r_1^{l+2}}{a^{l+2}}j_l(k_{nl}r_1)\sin(\omega_{nl}t)+\frac{en_e}{m}\sqrt{4\pi/3}[E_z(\boldsymbol{R},t)Y_{10}(\Omega)$$
$$+\sqrt{2}E_x(\boldsymbol{R},t)Y_{11}(\Omega)+\sqrt{2}E_y(\boldsymbol{R},t)Y_{1-1}(\Omega)], \tag{A10}$$

where $\omega_{0l}^2=\omega_p^2(l/2l+1)$. In derivation of the above equation the following formulae were exploited, (for $a<r_1$),

$$\frac{\partial}{\partial a}\frac{1}{\sqrt{a^2+r_1^2-2ar_1\cos\gamma}}=\frac{\partial}{\partial a}\sum_{l=0}^{\infty}\frac{a^l}{r_1^{l+1}}P_l(\cos\gamma)$$
$$=\sum_{l=0}^{\infty}\frac{la^{l-1}}{r_1^{l+1}}P_l(\cos\gamma), \tag{A11}$$

where $P_l(\cos\gamma)$ is the Legendre polynomial $[P_l(\cos\gamma)=4\pi/(2l+1)\Sigma_{m=-l}^{l}Y_{lm}(\Omega)Y_{lm}^*(\Omega_1)]$, γ is an angle between vectors $\boldsymbol{a}=a\hat{\boldsymbol{r}}$ and $\boldsymbol{r}_1$, and (for $a>r_1$),

$$\frac{\partial}{\partial a}\frac{1}{\sqrt{a^2+r_1^2-2ar_1\cos\gamma}}$$
$$=\frac{\partial}{\partial a}\sum_{l=0}^{\infty}\frac{r_1^l}{a^{l+1}}P_l(\cos\gamma)$$
$$=-\sum_{l=0}^{\infty}\sum_{m=-l}^{l}4\pi\frac{l+1}{2l+1}\frac{r_1^l}{a^{l+2}}Y_{lm}(\Omega)Y_{lm}^*(\Omega_1). \tag{A12}$$

Taking into account the spherical symmetry, one can assume the solution of the Eq. (A10) in the form,

$$\sigma(\Omega,t)=\sum_{l=0}^{\infty}\sum_{m=-l}^{l}q_{lm}(t)Y_{lm}(\Omega). \tag{A13}$$

From the condition $\int\sigma(\omega t)d\Omega=0$ it follows that $q_{00}=0$. Taking into account the initial condition $\sigma(\omega,0)=0$ we get (for $l\geq 1$),

$$q_{lm}(t)=\frac{B_{lm}}{a^2}\sin(\omega_{0l}'t)e^{-t/\tau_0}(1-\delta_{l1})+Q_{1m}(t)\delta_{l1}$$
$$+\sum_{n=1}^{\infty}A_{lmn}\frac{(l+1)\omega_p^2}{l\omega_p^2-(2l+1)\omega_{nl}^2}n_e$$
$$\times\int_0^a dr_1\frac{r_1^{l+2}}{a^{l+2}}j_l(k_{nl}r_1)\sin(\omega_{nl}'t)e^{-t/\tau_0}, \tag{A14}$$

where $\omega_{0l}'=\sqrt{\omega_{0l}^2-1/\tau_0^2}$ and $Q_{1m}(t)$ satisfies the equation,

$$\frac{\partial^2Q_{1m}(t}{\partial t^2}+\frac{2}{\tau_0}\frac{\partial Q_{1m}(t)}{\partial t}+\omega_{01}^2Q_{1m}(t)$$
$$=\frac{en_e}{m}\sqrt{4\pi/3}[E_z(\boldsymbol{R},t)\delta_{m0}+\sqrt{2}E_x(\boldsymbol{R},t)\delta_{m1}$$
$$+\sqrt{2}E_y(\boldsymbol{R},t)\delta_{m-1}]. \tag{A15}$$

Thus $\sigma(\omega,t)$ attains the form,

$$\sigma(\Omega,t)=\sum_{l=2}^{\infty}\sum_{m=-l}^{l}Y_{lm}(\Omega)\frac{B_{lm}}{a^2}\sin(\omega_{0l}'t)e^{-t/\tau_0}$$
$$+\sum_{m=-1}^{1}Q_{1m}(t)Y_{1m}(\Omega)$$
$$+\sum_{l=1}^{\infty}\sum_{m=-l}^{l}\sum_{n=1}^{\infty}A_{nlm}\frac{(l+1)\omega_p^2}{l\omega_p^2-(2l+1)\omega_{nl}^2}Y_{lm}(\Omega)n_e$$
$$\times\int_0^a dr_1\frac{r_1^{l+2}}{a^{l+2}}j_l(k_{nl}r_1)\sin(\omega_{nl}'t)e^{-t/\tau_0}. \tag{A16}$$

[1] S. Pillai, K. B. Catchpole, T. Trupke, G. Zhang, J. Zhao, and M. A. Green, Appl. Phys. Lett. **88**, 161102 (2006).
[2] M. Westphalen, U. Kreibig, J. Rostalski, H. Lüth, and D. Meissner, Sol. Energy Mater. Sol. Cells **61**, 97 (2000); M. Grätzel, J. Photochem. Photobiol. C **4**, 145 (2003).
[3] H. R. Stuart and D. G. Hall, Appl. Phys. Lett. **73**, 3815 (1998); Phys. Rev. Lett. **80**, 5663 (1998); H. R. Stuart and D. G. Hall, Appl. Phys. Lett. **69**, 2327 (1996).
[4] D. M. Schaadt, B. Feng, and E. T. Yu, Appl. Phys. Lett. **86**, 063106 (2005).
[5] K. Okamoto, I. Niki, A. Shvartser, Y. Narukawa, T. Mukai, and A. Scherer, Nature Mater. **3**, 601 (2004); K. Okamoto, I. Niki, A. Scherer, Y. Narukawa, T. Mukai, and Y. Kawakami, Appl. Phys. Lett. **87**, 071102 (2005).
[6] C. Wen, K. Ishikawa, M. Kishima, and K. Yamada, Sol. Energy Mater. Sol. Cells **61**, 339 (2000).
[7] L. Lalanne and J. P. Hugonin, Nat. Phys. **2**, 551 (2006).
[8] A. V. Zayats, I. I. Smolyaninov, and A. A. Maradudin, Phys. Rep. **408**, 131 (2005).
[9] S. A. Mayer, *Plasmonics: Fundamentals and Applications* (Springer, Berlin, 2007).
[10] W. L. Barnes, A. Dereux, and T. W. Ebbesen, Nature (London) **424**, 824 (2003).
[11] N. Engheta, A. Salandrino, and A. Alu, Phys. Rev. Lett. **95**, 095504 (2005).
[12] S. A. Maier and H. A. Atwater, J. Appl. Phys. **98**, 011101 (2005).
[13] G. Mie, Ann. Phys. **25**, 377 (1908).
[14] M. Brack, Phys. Rev. B **39**, 3533 (1989).
[15] L. Serra, F. Garcias, M. Barranco, N. Barberan, and J. Navarro, Phys. Rev. B **41**, 3434 (1990).
[16] M. Brack, Rev. Mod. Phys. **65**, 677 (1993).
[17] W. Ekardt, Phys. Rev. Lett. **52**, 1925 (1984).

[18]C. F. Bohren and D. R. Huffman, *Absorption and Scattering of Light by Small Particles* (Wiley, New York, 1983); U. Kreibig and M. Vollmer, *Optical Properties of Metal Clusters* (Springer, Berlin, 1995); J. I. Petrov, *Physics of Small Particles* (Nauka, Moscow, 1984); C. Burda, X. Chen, R. Narayanan, and M. El-Sayed, Chem. Rev. (Washington, D.C.) **105**, 1025 (2005).
[19]D. Pines, *Elementary Excitations in Solids* (ABP, Massachusetts, 1999).
[20]E. Prodan and P. Nordlander, Nano Lett. **3**, 543 (2003); E. Prodan, P. Nordlander, and N. J. Halas, *ibid.* **3**, 1411 (2003).
[21]E. Prodan and P. Nordlander, Chem. Phys. Lett. **352**, 140 (2002); E. Prodan, A. Lee, and P. Nordlander, *ibid.* **360**, 325 (2002).
[22]L. Jacak, J. Krasnyj, and A. Chepok, Fiz. Nizk. Temp. **35**, 491 (2009); W. Jacak, J. Krasnyj, J. Jacak, R. Gonczarek, A. Chepok, L. Jacak, D. Z. Hu, and D. Schaadt, J. Appl. Phys. **107**, 124317 (2010).
[23]D. Pines and D. Bohm, Phys. Rev. **85**, 338 (1952); D. Bohm and D. Pines, *ibid.* **92**, 609 (1953).
[24]A. Rubio and L. Serra, Phys. Rev. B **48**, 18222 (1993).
[25]L. D. Landau and E. M. Lifshitz, *Field Theory* (Nauka, Moscow, 1973) in Russian.
[26]M. L. Brongersma, J. W. Hartman, and H. A. Atwater, Phys. Rev. B **62**, R16356 (2000).
[27]U. Kreibig and L. Genzel, Surf. Sci. **156**, 678 (1985).
[28]C. Yannouleas, R. A. Broglia, M. Brack, and P. F. Bortignon, Phys. Rev. Lett. **63**, 255 (1989); G. Weick, G. L. Ingold, R. A. Jalabert, and D. Weinmann, Phys. Rev. B **74**, 165421 (2006).
[29]F. Stietz, J. Bosbach, T. Wenzel, T. Vartanyan, A. Goldmann, and F. Träger, Phys. Rev. Lett. **84**, 5644 (2000).
[30]M. Scharte, R. Porath, T. Ohms, M. Aeschlimann, J. R. Krenn, H. Ditlbacher, F. R. Aussenegg, and A. Liebsch, Appl. Phys. B: Lasers Opt. **73**, 305 (2001).
[31]F. J. García de Abajo, Rev. Mod. Phys. **82**, 209 (2010).
[32]F. J. García de Abajo, J. Phys. Chem. C **112**, 17983 (2008).
[33]S. A. Maier, P. G. Kik, and H. A. Atwater, Phys. Rev. B **67**, 205402 (2003).
[34]I. S. Gradstein and I. M. Rizik, *Tables of Integrals* (Fizmatizdat, Moscow, 1962).
[35]V. A. Markel and A. K. Sarychev, Phys. Rev. B **75**, 085426 (2007).
[36]E. Hao, R. C. Bayley, G. C. Schatz, J. T. Hupp, and S. Li, Nano Lett. **4**, 327 (2004).
[37]B. Lambrecht, A. Leitner, and F. R. Aussenegg, Appl. Phys. B: Lasers Opt. **64**, 269 (1997).